

Peristaltic Transport Of Casson Fluid In A Vertical Permeable Channel With Suction And Injection By Numerical Technique

K.Chakradhar ¹, K.Nandagopal ², G.Bhagyalaxmi³, V. Prashanthi³

1. Department of Humanities & Sciences, Kommuri Prathap Reddy Institute of Technology, Hyderabad, Telangana, India.
2. Department of Basic Sciences and Humanities, Sree Vidyanikethan Engineering College, A.Rangampet, Andhra Pradesh, India
3. Department of Humanities & Sciences, Kommuri Prathap Reddy Institute of Technology, Hyderabad, Telangana, India
DOI: 10.47750/pnr.2022.13.S08.54

Abstract

The peristaltic transport of a Casson fluid in a vertical permeable channel with suction and injection by Galerkin method is studied. The mathematical modeling is realized with an approximation of the extended wave length and a low Reynolds number. The mathematical solution is obtained for the velocity field, pressure gradient, frictional force within the reference wave system over one wavelength. The results of various parameters on pressure rise characteristics and frictional forces are discussed graphically. It is observed that the pressure rise decreases because the slip parameters and suction/injection parameter increases and increases because the amplitude increases.

Key words: Casson fluid, Galerkin method, slip parameters, permeability, suction and injection.

1. Introduction

peristalsis has attracted much attention of a large number of researchers due to its importance in engineering and medical applications. Peristalsis is an innate property of several biological systems and it occurs in the movement of urine from the kidney to bladder, vasomotion of small blood vessels, ovum transport in the fallopian tube and movement of chyme in the gastro-intestinal tract. It is an important transport mechanism not only in physiological processes but has a wide range of applications in engineering and industry. The principle of peristalsis has been used to develop pumps having physiological and industrial applications

Peristaltic transport is a progressive wave of area contraction or expansion along the length of a distensible tube, mixing and transporting the fluid in the direction of the wave propagation. To understand the behaviour of peristaltic, quite a lot of theoretical and experimental attempts have been made since the investigation of Latham [1]. A detailed review on peristalsis was presented by Jaffrin and Shapiro[2]. Fung and Tang [3] investigated longitudinal dispersion of particles in the blood flowing in a pulmonary alveolar. Thereafter quite a good number of analytical/ numerical studies pertaining to the flow of a Newtonian fluids were considered by many researchers in different physical constraints (Mishra et al. [4], Elshahawey et al. [5], Hayat .et al. [6], Nadeem and Akbar [7], Ramana Kumari and Radhakrishnamacharya[8]).

Blood being suspension of cells behaves like a Newtonian fluid when it flows through tubes (arteries) with larger diameter at higher shear rate. But it exhibits Non-Newtonian characteristics when it flows through tubes with small diameter at low shear rates. In view of this Casson model which is a yield stress model is widely used to explain the remarkable behaviour of blood flow through small blood vessels at low shear rates. In the area of constant flow of incompressible viscous fluid over infinite porous plates subject to suction or injection. Many authors have studied various aspects of the matter. Nandagopal et al. [9] discussed Couette flow of a Bingham fluid in a channel bounded by permeable beds with suction and injection.

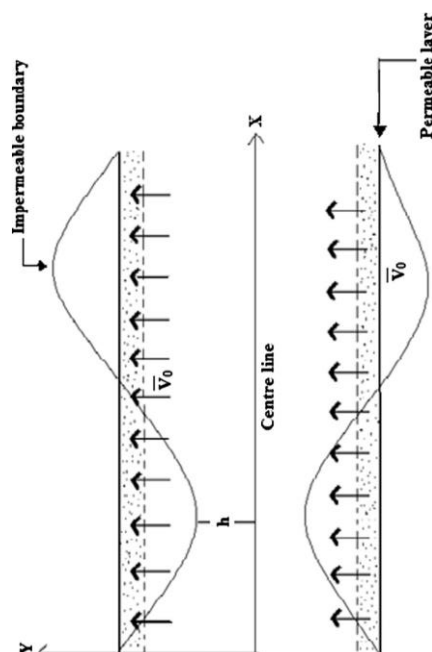
Casson fluid model describes the flow characteristics of blood more accurately at low shear rates and when it flows through small blood vessels. Keeping in view, Jayaraman et al. [10] extended Oka's work and suggested that Casson fluids are found to be more practically applicable in developing models for blood Oxygenators. Habtu and Radhakrishnamacharya [11] studied the effect of peristalsis on dispersion in a micropolar fluid. The flow of non Newtonian fluids in elastic inflatable and collapsible tubes is important to biofluid mechanics encountered in human body and other applications; The mechanisms of pharyngeal, oesophageal and intestinal transport of food and liquids is very useful for the treatment of patients with malfunctioning of these transport processes. Nandagopal et al. [12] studied Peristaltic motion of Pseudoplastic fluid in an inclined channel bounded by permeable walls.

Anil Kumar, Aggarwal SP [13] approaches Galerkin method for viscous incompressible fluid flow through a porous medium in Coaxial Cylinders. Masakazu Shibahara, S.N. Atluri [14] approaches local Petrov-Galerkin method for the analysis of heat conduction due to moving heat source in welding. Ahamad B, Khan, Ahamad S [15] used Galerkin finite element analysis for peristaltic flow of micro polar fluid through porous soaked inclined tube independent of wavelength. Chakradhar K et al. [16] investigates peristaltic motion of a viscous fluid in a porous channel with suction and injection by using Numerical technique (Galerkin method)

In this paper the peristaltic flow of a Casson fluid in a vertical channel with suction and injection through Galerkin method is investigated, under long wavelength and low Reynolds number assumptions. The fluid is injected into the channel perpendicular to the lower porous layer with constant velocity V_0 and is sucked bent to the upper permeable layer with the identical velocity V_0 , the speed, the pressure rise and friction forces are obtained. The results are obtained and discussed.

2. Mathematical formulation

Consider the peristaltic transport of a Casson fluid in a vertical channel with permeable walls of half width 'a'. A longitudinal train of progressive sinusoidal waves occurs on the upper and lower permeable walls of the channel. The fluid with a constant velocity V_0 is injected into the channel perpendicular to the lower permeable wall and is sucked out of the upper permeable wall with the same velocity V_0 : For simplicity, we consider our discussion to half width of the channel as shown in Fig.



The wall deformation is given by

$$H(X, t) = a + b \sin \frac{2\pi}{\lambda} (x - ct) \quad (1)$$

where b is the amplitude, λ is the wavelength and c is the wave speed. Under the assumptions that the channel length is an integral multiple of the wavelength λ and the pressure difference across the ends of the channel is a constant, the flow becomes steady in the wave frame (x, y) moving with velocity c away from the fixed laboratory frame (X, Y) .

The transformation between these two frames is given by

$$x = X - ct, \quad y = Y, \quad u(x, y) = U(X - ct, Y); \quad v(x, y) = V(X - ct, Y) \quad (2)$$

we use the following non-dimensional quantities

$$\bar{x} = \frac{x}{\lambda}, \quad \bar{y} = \frac{y}{a}, \quad \bar{t} = \frac{ct}{\lambda}, \quad \bar{\phi} = \frac{b}{a}, \quad \bar{Q}_1 = \frac{Q_1}{c}, \quad \bar{v}_0 = \frac{v_0}{c}, \quad \bar{u} = \frac{u}{c}, \quad \text{Re} = \frac{\rho ac}{\mu}$$

$$\bar{p} = \frac{2\pi a^2}{\lambda c \mu} p, \quad \delta = \frac{2\pi a}{\lambda}, \quad \beta_1 = \frac{\alpha}{a}, \quad \beta_2 = \frac{\alpha}{a^2} \quad (3)$$

where R_e is Reynolds number, ϕ is the amplitude ratio, β is the permeability (including slip) parameter, and k is the suction parameter. The equations governing the motion in non dimensional form are

$$\left(1 + \frac{1}{\beta}\right) \frac{\partial^2 u}{\partial y^2} - k \frac{\partial u}{\partial y} + \eta = P \quad (4) \quad \text{where}$$

$$k = R_e V_o, \quad \text{and } P = \frac{\partial p}{\partial x}, \quad \beta \text{ is the Casson fluid parameter } Q_1 = \frac{P}{\sigma^2} \text{ (Darcy's law)} \quad (5)$$

The non-dimensional boundary conditions are

$$\frac{\partial u}{\partial y} = 0 \quad \text{at } y = 0 \quad (6)$$

$$u = -1 - \beta_1 \frac{\partial u}{\partial y} - \beta_2 \frac{\partial^2 u}{\partial y^2} \quad \text{at } y = h \quad (7)$$

Eq. (7) represents the complete slip boundary condition at the permeable wall in which β_1 is the first order slip parameter and β_2 is the second order slip parameter

3. Solution

Solving Eq. (4) using Galerkin method with the boundary conditions (6) and (7), we obtain the velocity as

$$u = -1 + a_2(y^2 - h^2 - 2\beta_1 h - 2\beta_2) + a_3(y^3 - h^3 - 3\beta_1 h^2 - 6\beta_2 h) \quad (8)$$

$$\text{Where } a_2 = P \left(\frac{B_1 C_2 - B_2 C_1}{A_1 B_2 - A_2 B_1} \right) \quad a_3 = P \left(\frac{A_2 C_1 - A_1 C_2}{A_1 B_2 - A_2 B_1} \right) \quad \text{and}$$

$$A_1 = k \left(\frac{h^4}{2} + 2\beta_1 h^3 + 2\beta_2 h^2 \right) - \left(1 + \frac{1}{\beta} \right) \left(\frac{4h^3}{3} + 4\beta_1 h^2 + 2\beta_2 h \right)$$

$$B_1 = k \left(\frac{2h^5}{5} + 2\beta_1 h^4 + 2\beta_2 h^3 \right) - \left(1 + \frac{1}{\beta} \right) \left(\frac{3h^3}{2} + 6\beta_1 h^3 + 6\beta_2 h^2 \right)$$

$$C_1 = \frac{2h^3}{3} + 2\beta_1 h^2 + 2\beta_2 h$$

$$A_2 = k \left(\frac{3h^5}{5} + 3\beta_1 h^4 + 6\beta_2 h^3 \right) - \left(1 + \frac{1}{\beta} \right) \left(\frac{3h^4}{2} + 6\beta_1 h^3 + 12\beta_2 h^2 \right)$$

$$B_2 = k \left(\frac{h^6}{2} + 3\beta_1 h^5 + 6\beta_2 h^4 \right) - \left(1 + \frac{1}{\beta} \right) \left(\frac{9h^5}{5} + 9\beta_1 h^4 + 18\beta_2 h^3 \right)$$

$$C_2 = \frac{3h^4}{4} + 2\beta_1 h^3 + 6\beta_2 h^2$$

The volume flux q through each cross section in the wave frame is given by

$$q = \int_0^h u dy = -h - a_2 \left(\frac{2h^3}{3} + 2\beta_1 h^2 + 2\beta_2 h \right) - a_3 \left(\frac{3h^4}{4} + 3\beta_1 h^3 + 6\beta_2 h^2 \right) \quad (9)$$

The instantaneous volume flow rate $Q(X, t)$ in the laboratory frame between the central line and the wall is

$$Q(X, t) = \int_0^H U(X, Y, t) dY = -a_2 \left(\frac{2h^3}{3} + 2\beta_1 h^2 + 2\beta_2 h \right) - a_3 \left(\frac{3h^4}{4} + 3\beta_1 h^3 + 6\beta_2 h^2 \right) \quad (10)$$

From Eq. (9) we have,

$$\frac{dP}{dx} = \frac{(q + h)(A_1 B_2 - A_2 B_1)}{G_1 (B_1 C_2 - B_2 C_1) + G_2 (A_2 C_1 - A_1 C_2)} \quad (11)$$

where

$$G_1 = -\left(\frac{2h^3}{3} + 2\beta_1 h^2 + 2\beta_2 h\right)$$

$$G_2 = -\left(\frac{3h^4}{4} + 3\beta_1 h^3 + 6\beta_2 h^2\right)$$

The time average flux \bar{Q} over one period of the peristaltic wave is

$$\bar{Q} = \frac{1}{T} \int_0^T Q dt = q + 1 \quad (12)$$

4. The pumping characteristics

Integrating Eq. (11) with respect to x over one wavelength, we get the pressure rise (drop) over one cycle of the wave is

$$\Delta P = \int_0^1 \frac{(q+h)(A_1 B_2 - A_2 B_1)}{G_1(B_1 C_2 - B_2 C_1) + G_2(A_2 C_1 - A_1 C_2)} dx \quad (13)$$

The dimensionless friction force F at the wall across one wavelength is given by

$$F = \int_0^1 h \left(-\frac{dP}{dx}\right) dx \quad (14)$$

5. Results and discussion

In this section the graphical result of the casson fluid model is presented. The expressions for pressure rise and friction forces are calculated using numerical technique. The pressure rise for fluid increases by increasing amplitude ratio in the region of peristaltic pumping whereas it shows opposite behaviour in the co-pumping region.

In fig 2, the pressure rise ΔP with respective time average flow rate \bar{Q} increases as amplitude ratio increases with fixed values of slip parameters, casson fluid parameter, suction parameter

In fig 3, the pressure rise ΔP with respective time average flow rate \bar{Q} decreases as suction parameter increases with fixed values of amplitude ratio, slip parameters, casson fluid parameter, suction parameter

In fig 4, the pressure rise ΔP with respective time average flow rate \bar{Q} decreases as slip parameter ' β_1 ' increases with fixed values of amplitude ratio, suction parameter, casson fluid parameter.

In fig 5, the pressure rise ΔP with respective time average flow rate \bar{Q} decreases as slip parameter ' β_2 ' increases with fixed values of amplitude ratio, suction parameter, casson fluid parameter

Frictional force F

From Eq. (14), the frictional force F is calculated from Figs. 6–9, it is observed that the frictional force shows opposite behaviour compared to the pressure rise.

In fig.6, the frictional force F with respective time average flow rate \bar{Q} increases as of amplitude ratio increases with fixed values of slip parameters, casson fluid parameter, suction parameter

In fig.7, the frictional force F with respective time average flow rate \bar{Q} decreases as suction parameter increases with fixed values of amplitude ratio, slip parameters, casson fluid parameter,

In fig 8, the frictional force F with respective time average flow rate \bar{Q} decreases as slip parameter β_1

increases with fixed values of amplitude ratio, suction parameter

In fig 9, the frictional force F with respective time average flow rate \bar{Q} decreases as slip parameter β_2 increases with fixed values of amplitude ratio, suction parameter

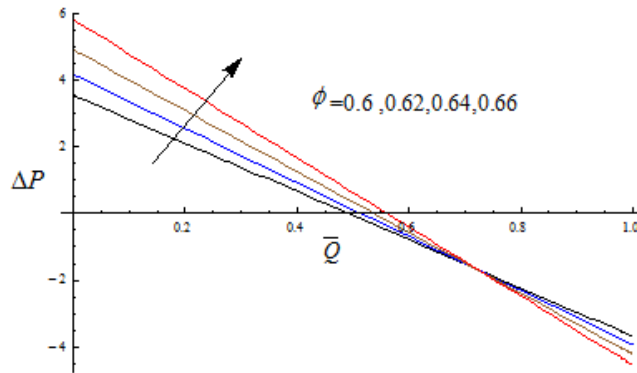


Fig 2. The change of pressure rise ΔP against time average volume flow rate \bar{Q} for different values of ϕ with fixed $\beta = 20$, $\beta_1 = 0.004$, $\beta_2 = 0.004$, $k = 1.5$, $\eta = 0.1$.

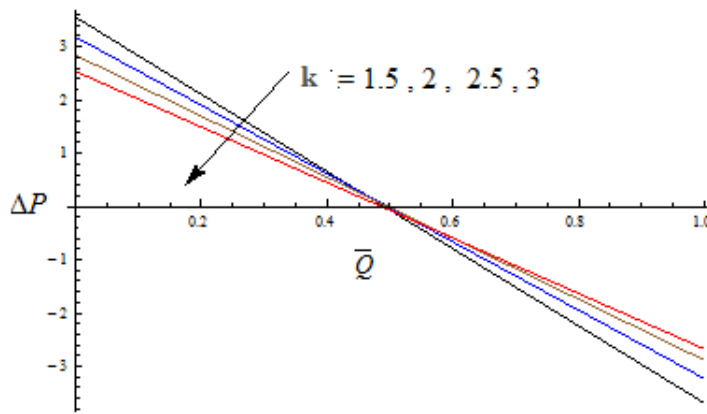


Fig 3. The change of pressure rise ΔP against time average volume flow rate \bar{Q} for different values of k with fixed $\phi = 0.6$, $\beta = 20$, $\beta_1 = 0.004$, $\beta_2 = 0.004$, $\eta = 0.1$.

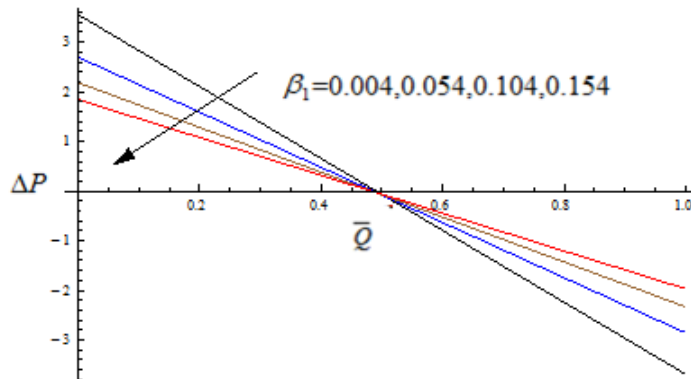


Fig 4. The change of pressure rise ΔP against time average volume flow rate \bar{Q}

for different values of β_1 with fixed $\phi=0.6$, $\beta=20$, $\beta_2=0.004$, $k=1.5$, $\eta=0.1$.

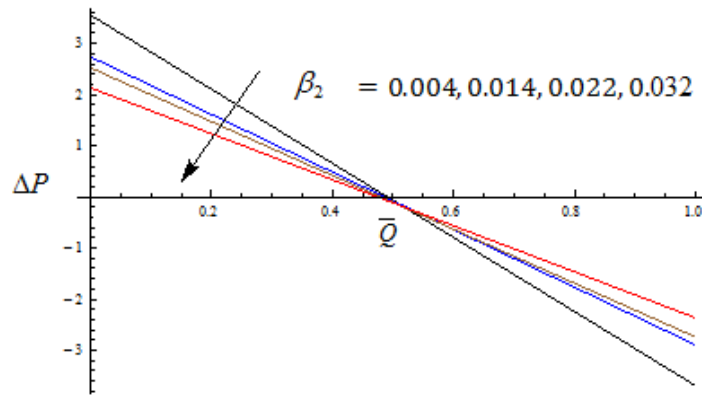


Fig 5. The change of pressure rise ΔP against time average volume flow rate \bar{Q} for different values of β_2 with fixed $\phi=0.6$, $\beta=20$, $\beta_1=0.004$, $k=1.5$, $\eta=0.1$.

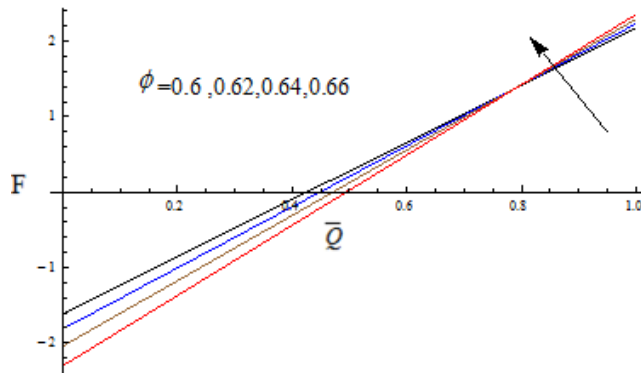


Fig 6. The change of Frictional force F against time average volume flow rate \bar{Q} for different values of ϕ with fixed $\beta=20$, $\beta_1=0.004$, $\beta_2=0.004$, $k=1.5$, $\eta=0.1$.

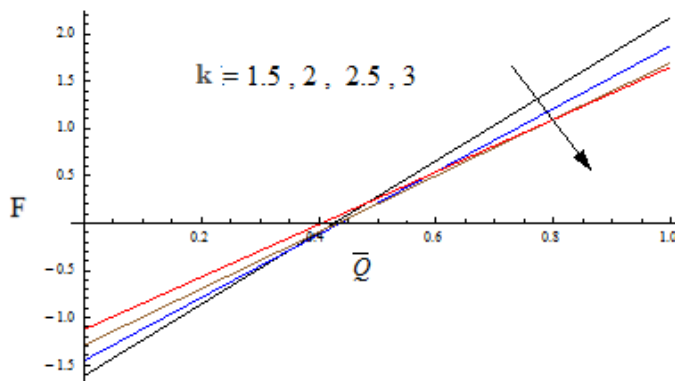


Fig 7. The change of Frictional force F against time average volume flow rate \bar{Q}

for different values of k with fixed $\phi=0.6$, $\beta=20$, $\beta_1=0.004$, $\beta_2=0.004$, $\eta=0.1$.

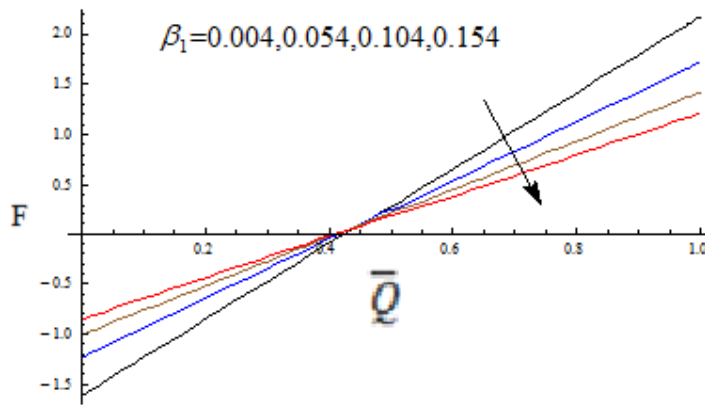


Fig 8. The change of Frictional force F against time average volume flow rate \bar{Q} for different values of β_1 with fixed $\phi=0.6$, $\beta=20$, $\beta_2=0.004$, $k=1.5$, $\eta=0.1$

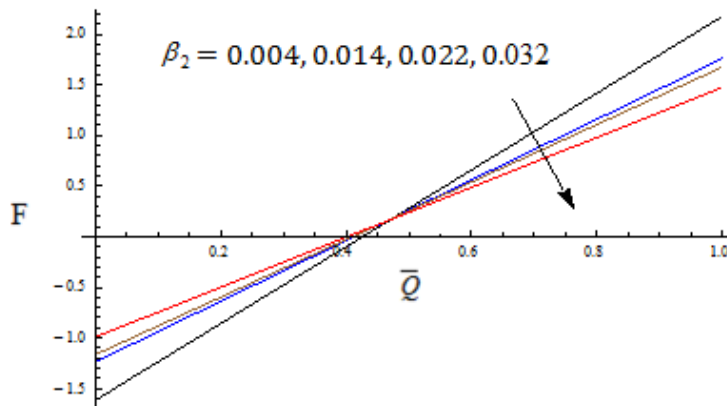


Fig 9. The change of Frictional force F against time average volume flow rate \bar{Q} for different values of β_2 with fixed $\phi=0.6$, $\beta=20$, $\beta_1=0.004$, $k=1.5$, $\eta=0.1$.

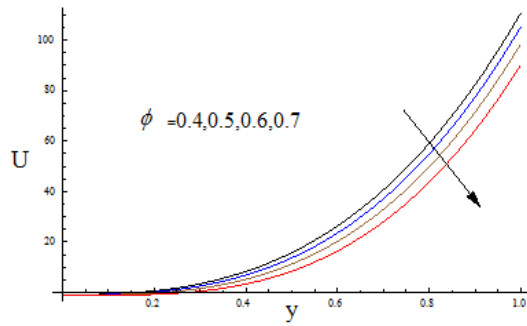


Fig10(a)

Velocity profile for different amplitude ratios

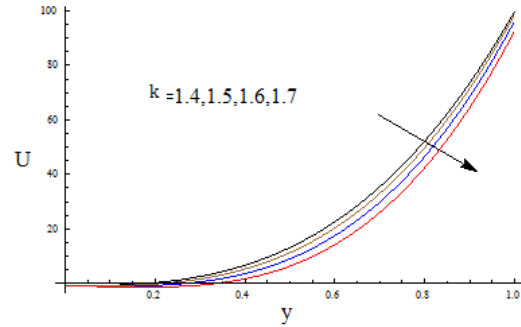


Fig10(b)

Velocity profile for different suction parameters

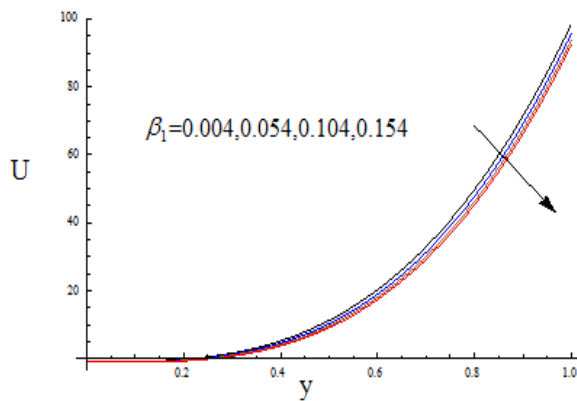


Fig10(c)

Velocity profile for different first order slip Parameters

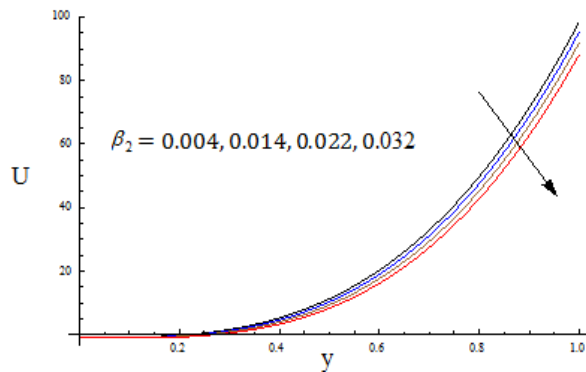


Fig10(d)

Velocity profile for different second order slip parameters

Velocity Distribution.

Variation of velocity for various values of flow rate and amplitude ratio has been presented in Fig.10(a) - 10(d). For casson fluid, the magnitude of velocity is noticed to be highest in channel. The magnitude of velocity decreases with an increasing values in amplitude ratio and various parameters.

Fig.10(a) illustrates the velocity distribution against y for several values of the amplitude ratios. It is found that the increase in the amplitude ratio decreases to the velocity of the flow field.

In fig. 10(b). It is observed that the increase in the suction parameter decreases to the velocity of the flow field .

Fig.10 (c & d) illustrates the velocity distribution against y for several values of the slip parameters. It is found that increase in the slip parameter decreases to the velocity of the flow field.

6. Conclusion

The Peristaltic transport of a casson fluid in a vertical channel with suction and injection has been studied in the present work under the assumption of long wavelength and low Reynolds number approximations. The expressions for velocity field, pressure rise and frictional force are determined. It is observed that decreases the pressure rise. as increase in the suction/injection parameter and increase in the slip parameters, also the pressure rise increase with increase in the amplitude ratio .The frictional force shows opposite behaviour to that of pressure rise .

References

- [1] Latham, T.W. Fluid motion in a peristaltic pump. M.S. Thesis, M. I. T. Massachusetts Institute of Technology, Cambridge, (1966); 1-74.
- [2] Jaffrin M. Y., Shapiro A.H. Peristaltic pumping. *Annu Rev. Fluid Mech*, (1971); (3), 13–36.
- [3] Fung M.Y., Tang H.T. Longitudinal dispersion of particles in the blood flowing in a pulmonary alveolar sheet. *J. Appl. Mech.*, (1975); 42, (5), 36–40.
- [4] Mishra, M. and Rao, A. R. Peristaltic transport of a Newtonian fluid in an asymmetric channel. *ZAMP* (2004); (54), 532-550.
- [5] Elshehawey, E. F., Eladabe, N.T., Elghazy, E.M. and Ebaid, A., Peristaltic transport in an asymmetric channel through a porous medium . *Appl. Math. Comput.*, (2006); 182, 140-150.
- [6] Hayat, T., Ali, N., Asghar, S., and Siddiqui A.M.. Exact peristaltic flow in tubes with endoscope. *Appl. Math. Comput.*,(2006); (182), 359-368.
- [7] Nadeem, S. and Akbar N.S. Effects of heat transfer on the peristaltic transport of MHD Newtonian fluid with variable viscosity:application of a domain decomposition method.*CNSNS*. (2009a); (14), 3844 - 3855.
- [8] Ramanakumari A.V. and Radhakrishnamacharya G. Effect of slip on Heat Transfer to Peristaltic Transport in the presence of Magnetic Field with Wall Effects. *ARPJ Journal of Engineering and Applied Sciences* (2011); 6 (7), 118-131.
- [9] Nandagopal. K , Sreenadh .S, and Chakradhar. K. Couette Flow of a Bingham Fluid in a Channel Bounded By Permeable Beds with suction and Injection, *IJESRT*, (2014); 3(9), 300-305.
- [10] Jayaraman, G., Lautier, A., Jarry. Bui-Mong-Hang A.G..and Salzman E.W. Numerical scheme for modeling oxygen transfer in tubular oxygenators. *Med., and Biol., Engng and Compt.* (1981); 19, 524-534.
- [11] Habtu, A. and Radhakrishnamacharya, G. The Effect of Peristalsis on Dispersion in a micropolar fluid. *World Academy of Sciences, Engineering and Technology.* (2011); (51), 1041-1047.
- [12] Nandagopal. K, Chakradhar. K., Nagender. Ch., Sastry. T.V.A.P., Peristaltic motion of pseudoplastic fluid in an inclined channel bounded by permeable walls. *IJARES* (2022); 10 (3), 1312-1325.
- [13] Anil Kumar, Agarwal SP , Finite Element Galerkin’s Approach for Viscous Incompressible Fluid Flow through a Porous Medium in Coaxial Cylinders. *Journal of Mathematical Sciences and Applications.* (2013); 1 (3), 39-42 .
- [14] Masakazu Shibahara, Atluri S N , The mesh less local Petrov-Galerkin method for the analysis of heat conduction due to a moving heat source in welding . *International Journal of Thermal Sciences.* (2011); 50 (6), 984-992.
- [15] Ahmad B., Khan S.U., Ahmad S, Galerkin finite element analysis for peristaltic flow of micropolar fluid through porous soaked inclined tube independent of wavelength , *ARCHIVE Proceedings of the Institution of Mechanical Engineers Part. E. .Journal of Process of Mechanical Engineering.* (2021)
- [16] Chakradhar. K . Nanda Gopal. K , Bhagyaxmi. G, Investigation of peristaltic motion of viscous fluid in a porous channel with Suction and Injection by using Numerical technique. (Galerkin method), *Specialusis ugdymas*, (2022); 1 (43), 4214-4222.